analytical chemistry

Article

pubs.acs.org/ac

Water-Soluble Conjugated Polymer as a Fluorescent Probe for Monitoring Adenosine Triphosphate Level Fluctuation in Cell Membranes during Cell Apoptosis and in Vivo

Binghuan Huang, Zhirong Geng,* Shihai Yan, Zan Li, Jun Cai, and Zhilin Wang*

State Key Laboratory of Coordination Chemistry, School of Chemistry and Chemical Engineering, Collaborative Innovation Center of Advanced Microstructure, Nanjing University, Nanjing, Jiangsu 210093, China

Supporting Information

ABSTRACT: Adenosine triphosphate (ATP) is used as the energy source in cells and plays crucial roles in various cellular events. The cellular membrane is the protective barrier for the cytoplasm of living cells and involved in many essential biological processes. Many fluorescent probes for ATP have been successfully developed, but few of these probes were appropriate for visualizing ATP level fluctuation in cell membranes during the apoptotic cell death process. Herein, we report the synthesis of a new water-soluble cationic polythiophene derivative that can be utilized as a fluorescent sensor for detecting ATP in cell membranes. Poly((3-((4-methylthiophen-3-yl)oxy)propyl)triphenylphosphonium chloride) (PMTPP) exhibits high sensitivity and good selectivity to ATP, and the detection limit is 27 nM. The polymer shows low toxicity to live cells and excellent photostability in cell membranes. PMTPP was practically utilized for real-time monitoring of ATP levels in the cell membrane through fluorescence microscopy. We have demonstrated that the ATP levels in cell membranes increased during the apoptotic cell death process. The probe was also capable of imaging ATP levels in living mice.

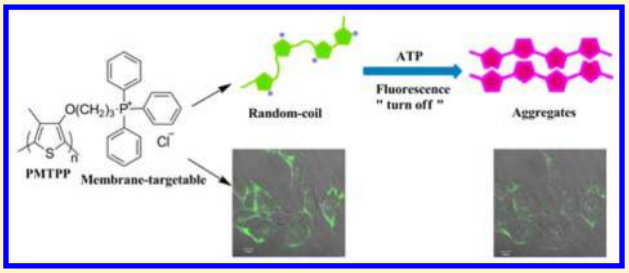

Adenosine triphosphate (ATP) is the primary energy source in cells and plays vital roles in many cellular events in living organisms. Cellular ATP has been used as an indicator for cell viability and cell injury[1] and a trigger for controlled release of anticancer drugs.[2,3] The cellular membrane is the protective barrier for the cytoplasm of living cells and involved in many essential biological processes, such as signal transduction, energy conversion, and transport of ions and molecules into and out of the cell.[4,5] In particular, the transport of ions and some molecules, such as Na^+, K^+, Ca^{2+}, amino acid, glucose, and DNA, is required for the utilization of ATP.[6−9] Therefore, visualization of ATP levels in cell membranes is critical to accurately assess the biological processes related to the plasma membrane. In addition, recent studies have shown that apoptotic stimuli induce significant elevation of cytosolic ATP levels and mitochondrial ATP levels.[10,11] However, to date, the change of ATP levels in the cell membrane during the apoptotic cell death process has not been investigated. Hence, it is necessary to develop useful tools for tracking and imaging ATP levels in cell membranes.

Several strategies, such as peptides,[12−14] aptamers,[15−28] ATP-dependent ligation,[29−33] and G-quadruplex-based luminescent assays,[34,35] have been developed to detect ATP. However, few of these methods have been utilized to determine the ATP level in cells. In recent years, fluorescent probes are considered as powerful tools for the identification of substances in biological systems because of the good selectivity, high sensitivity, low cost, simplicity, capability for real-time analysis, and high temporal and spatial resolution.[36−41] In particular, fluorescent chemosensors that can localize in a certain cellular region or organelle play pivotal roles in detection or imaging biological molecules in a specific region with high accuracy and low background noise. Recently, several organelle-targeting fluorescent ATP chemosensors, such as mitochondria-targeting sensors[11,42−44] and lysosome-targeting sensors,[45] have been reported. To the best of our knowledge, only one small-molecule fluorescent probe was synthesized for cell membrane ATP imaging,[42] but the probe lacks selectivity among various phosphate anions. Hence, there is a compelling need to develop a new fluorescent probe for monitoring ATP levels in cell membranes.

Among water-soluble conjugated polymers (CPs), water-soluble polythiophene (PT) derivatives have been confirmed to be highly sensitive fluorescent and colorimetric probes for the detection of DNA,[46−50] proteins,[51−53] and small molecules of biological interest.[45,54−61] Recently, several water-soluble PTs were prepared for live cell imaging because of their low toxicity, high fluorescence intensity, and good photostability.[45,61−66] However, water-soluble polythiophene derivatives were not utilized for tracking ATP levels in cell membranes.

Triphenylphosphonium (TPP) is a delocalized lipophilic cation and can be attracted by the negative potential of the

Received: April 1, 2017
Accepted: July 28, 2017
Published: July 28, 2017

DOI: 10.1021/acs.analchem.7b01212
Anal. Chem. 2017, 89, 8816−8821

inner membrane of living cells.[67] Moreover, the polythiophene backbone preferentially accumulates in hydrophobic membranes.[42] Herein, we synthesized a new water-soluble cationic polythiophene derivative with side chains bearing triphenylphosphonium groups, poly((3-((4-methylthiophen-3-yl)oxy)-propyl)triphenylphosphonium chloride) (PMTPP), using a $FeCl_3$ oxidative polymerization method (Scheme S1). We anticipated that PMTPP would adopt a random-coil conformation in water. It might form aggregates upon interacting with ATP (Scheme 1). PMTPP can localize to the cell membrane and has high sensitivity and good selectivity to ATP. The polymer exhibits low cytotoxicity and good photostability. PMTPP can be utilized as a fluorescent sensor for monitoring ATP levels in cell membranes during the apoptotic cell death process and in vivo.

Scheme 1. Proposed Fluorescent Sensing Mechanism of PMTPP to ATP

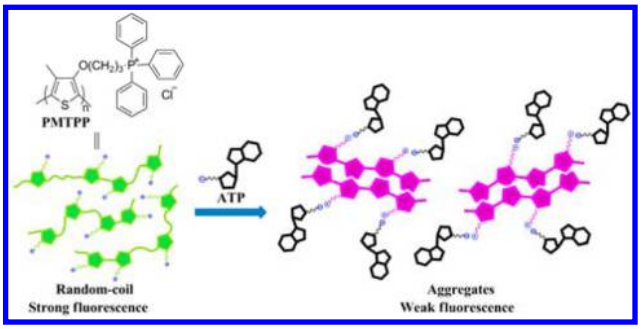

EXPERIMENTAL SECTION

Reagents and Instruments. DiI was purchased from Beyotime (Nanjing, China). The primary antibodies directed to β-actin (1:1000, CST) and [HRP-labeled goat anti-rabbit IgG(H+L)] secondary antibody (1:1000, CST) were used. The other reagents were bought from Alfa Aesar (Shanghai, China), Sigma-Aldrich (St. Louis, USA), J&K (Beijing, China), and Aladdin (Shanghai, China).

^1H NMR and ^{13}C NMR spectra were taken on a Bruker Avance DRX-500 (500 Hz) spectrometer. The mass spectra were measured on a LCQ Fleet spectrometer (ThermoFisher). The molecular weight was determined by an Agilent 1100. Transmission electron microscopy (TEM) data were measured on JEM-1011 (JEOL). The fluorescence spectra were collected on a PerkinElmer LS 55 spectrometer. Cell imaging was carried out by a LSM 710 microscope (Zeiss). The flow cytometry analysis was performed on a Microplate Reader (BD LSRFortessa). The in vivo images of mice were performed with a CRI Maestro Ex in vivo imaging system.

Synthesis of (3-((4-Methylthiophen-3-yl)oxy)propyl)-triphenylphosphonium Bromide (MTPP). Tripheylphosphine (1.41 g, 5.37 mmol) was added to a solution of 3-(3-bromopropoxy)-4-methylthiophene (MTPBr) (0.605 g, 2.57 mmol) dissolved in CH_3CN (25 mL). The contents were heated at 70 °C with stirring for 4 days. After workup, the resulting residue was recrystallized from a mixture of hexane/ethyl acetate to yield MTPP as yellow solid (0.4 g, 31%). ^1H NMR ($CDCl_3$, TMS, 500 MHz) δ 7.95−7.56 (15H, m), 6.79 (1H, t), 6.20 (1H, dd), 4.28 (2H, t), 4.03 (4H, dd), 2.19 (2H, t), 2.01 (3H, d). ^{13}C NMR ($CDCl_3$, TMS, 500 MHz) δ 12.82, 19.86, 22.95, 68.62, 97.80, 118.10, 120.11, 128.66, 130.61, 133.73, 135.17, 154.88. ESI MS (m/z): 417.33 $[M - Br]^+$.

Synthesis of Polymer PMTPP. A solution of MTPP (0.1 g, 0.2 mmol) in chloroform (3 mL) was added dropwise to a stirred solution of $FeCl_3$ (0.13 g, 0.81 mmol) in chloroform (4 mL) under N_2 atmosphere. The contents were heated at 35 °C with stirring for 5 days. After workup, the residue was washed two times with methanol. The crude product was dissolved in acetone and then precipitated by adding tetrabutylammonium chloride. Thereafter, the polymer was dissolved in methanol and dedoped by addition of hydrazine. The solvent was removed under vacuum condition, and the product was washed with acetone saturated with tetrabutylammonium chloride. The resulting polymer was dried under vacuum condition to yield PMTPP (0.049 g, 49%). Determination of the molecular weight of PMTPP was by gel permeation chromatography (GPC): M_n = 89.9 kDa, M_w = 104.6 kDa, and PD = 1.16 (M_n: number-average molecular weight; M_w: weight-average molecular weight; PD: polydispersity; 1 Da = 1 g/mol). S_{PMTPP} = 0.25 g/100 g water (S: solubility).

Cell Culture. HepG2 cells, HeLa cells, and HL 7702 cells were bought from the Cell Bank of the Chinese Academy of Sciences. The cells were cultured in Dulbecco's Modified Eagle Medium (DMEM) supplemented with 10% fetal bovine serum (FBS) and 1% penicillin/streptomycin in a humidified atmosphere of 5% CO_2 at 37 °C.

3-(4,5-Dimethyl-thiazoly)-2,5-diphenyltetrazolium Bromide (MTT) Assay. 2×10^4 cells were seeded into 96-well cell-culture plates, followed by incubation for 12 h at 37 °C. Thereafter, different amounts of PMTPP were added to each well, and wells were incubated for 24 h. Then, 20 μL of 0.5 mg/mL MTT was added to each well. After incubating the cells for 4 h, the medium was removed and 150 μL of DMSO was added to each well to dissolve the blue formazan. The absorbance was measured on an automatic enzyme-linked immunosorbent assay plate reader at a wavelength of 560 nm.

Cell Imaging. HepG2 cells, HeLa cells, and HL 7702 cells were seeded into cell-culture plates, followed by incubation for 12 h at 37 °C. Thereafter, PMTPP was added onto the plates, which were then incubated for 24 h at 37 °C. Cells stained with PMTPP were incubated with DiI for 30 min at 37 °C. Then, the medium was removed, and the cells were washed three times with PBS. Cell imaging was performed with a laser scanning confocal fluorescence microscope.

Flow Cytometric Assay. HepG2 cells were plated on 6-well plates for 12 h and then were stained with PMTPP for 24 h at 37 °C. The cells stained with PMTPP were washed with PBS and then were detached from the 6-well plates using Trypsin-EDTA solution. The solution containing treated cells was centrifuged (1000 rpm, 4 min) and resuspended in PBS three times. Flow cytometry analysis was performed with a Microplate Reader.

Western Blot Analysis. HepG2 cells were seeded into 6-well plates and incubated for 24 h at 37 °C under a 5% CO_2 atmosphere and then were treated with cisplatin (20 μM) for 0, 0.5, 1, 2, and 3 h. Cells were harvested and washed with ice cold PBS twice. The extracts of total cellular protein were obtained at 4 °C in lysis buffer containing 20 mM Tris-HCl (pH 8.0), 250 mM NaCl, 0.4 mM Na_3VO_4, 1% SDS, and 1× Complete mini protease inhibitor cocktail tablets. Samples were separated by 12% SDS-PAGE and transferred to an immobilon-P transfer membrane (Millipore, USA). Membranes were blocked with 5% nonfat milk in TBS containing 0.1% Tween 20 at room

DOI: 10.1021/acs.analchem.7b01212
Anal. Chem. 2017, 89, 8816−8821

temperature for 1 h and incubated with primary antibodies. The antibodies were diluted in TBS with 5% nonfat milk overnight at 4 °C. Then, the blots were incubated with an [HRP-labeled goat anti-rabbit IgG(H+L)] secondary antibody (1:4000) for 1 h at room temperature. Enhanced chemiluminescence (ECL, Millipore) was performed afterward.

In Vivo Imaging. Male nude mice were purchased from Beijing Vital River Laboratory Animal Technology Co., Ltd. at 8 weeks of age. All animal experiments were performed in accordance with the guidelines issued by The Ethical Committee of Nanjing University. For in vivo imaging, HepG2 cells (5×10^6 cells suspended in 100 μL of PBS) were inoculated into the right forelimb of the nude mice after anesthetization by injection of 4% chloral hydrate (150 μL). After inoculation for 2 weeks, the mice were chosen for in vivo imaging experiments with the tumor diameters reaching approximately 0.5 cm. HepG2 tumor-bearing nude mice were subcutaneously injected with PMTPP (250 μM, 100 μL in saline) near the tumor tissue and then were given i.p. cavity injection with cisplatin (20 μM, 200 μL in saline) for 30 min. The nude mice were imaged using a CRI Maestro Ex in vivo imaging system. The excitation filter and emission filter were set as 455 and 560 nm, respectively.

Preparation of Stock Solutions of PMTPP and Anions. Stock solutions of PMTPP and various anions were prepared in aqueous solution. Concentrations of adenosine monophosphate (AMP), adenosine diphosphate (ADP), and adenosine triphosphate (ATP) were measured with UV−vis spectra in 100 mM phosphate buffer solution with pH 7.0 ($\varepsilon_{259(\mathrm{AMP,\ ADP,\ ATP})} = 1.54 \times 10^4\ \mathrm{M^{-1}\ cm^{-1}}$).

General Fluorescence Spectra Measurements. Stock solutions of PMTPP were diluted to the required concentration (50 μM). During the titration, different concentrations of anions were, respectively, added into the PMTPP solution and the fluorescence spectra of PMTPP was collected at room temperature.

RESULTS AND DISCUSSION

Selectivity Studies of PMTPP toward ATP. Fluorescence responses of PMTPP to various biological anions were investigated. Figure 1 summarizes the emission decrease ratio (I_o/I at 524 nm) upon adding various anions including AMP, ADP, ATP, phosphate anions (PO_4^{3-}, HPO_4^{2-}, $H_2PO_4^-$), pyrophosphate (PPi), triphosphate ($P_3O_{10}^{5-}$), HCO_3^-, NO_3^-, F^-, Cl^-, Br^-, I^-, $CH_3CO_2^-$, AsO_2^-, and SO_4^{2-}. PMTPP shows good selectivity to ATP, and the emission at 524 nm undergoes a 4.0-fold decrease in fluorescence intensity in the presence of ATP. In contrast, other anionic species scarcely induced clear fluorescence alterations except for $P_3O_{10}^{5-}$ (1.5-fold). Moreover, the plasma membrane is a dynamic structure composed of various proteins, lipids, and other biomolecules. Thus, we also investigated the fluorescent response of PMTPP to bovine serum albumin (BSA), cysteine (Cys), glutamic acid (Glu), glutathione (GSH), lysine (Lys), and calf thymus DNA (CTDNA). As shown in Figure S1, the protein, DNA, biological thiols, and amino acids induced no changes in the fluorescence of PMTPP. In addition, the presence of common metal ions like Zn^{2+}, Mg^{2+}, Ca^{2+}, K^+, and Na^+ also created no interference with the detection of ATP (Figure S1).

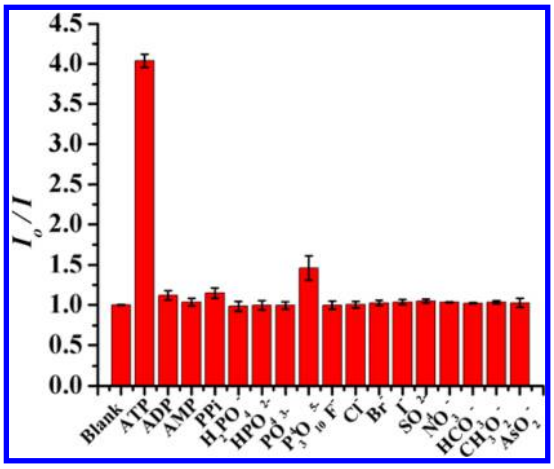

Figure 1. Fluorescence response of PMTPP (50 μM) to 5 μM of various anions in 10 mM HEPES buffer solution of pH 7.4. λ_{ex} = 410 nm.

Fluorescence Response of PMTPP to ATP. To investigate the fluorescence response of PMTPP to ATP, titration experiments were performed (Figure 2a). We observed

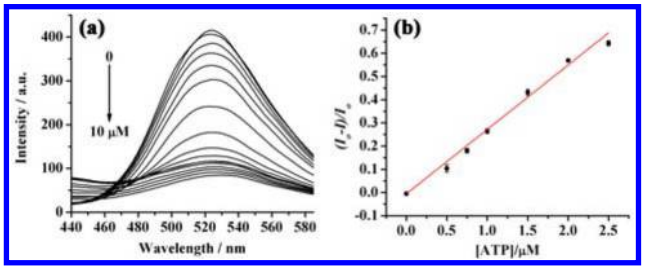

Figure 2. (a) Fluorescence spectral changes of PMTPP (50 μM) upon adding ATP in 10 mM HEPES buffer solution of pH 7.4 (λ_{ex} = 410 nm). (b) Linear plot of $(I_o - I)/I_o$ against concentrations of ATP.

that free PMTPP has a fluorescent emission maximum at 524 nm. Upon adding increasing concentrations of ATP, the fluorescence intensity of PMTPP decreases progressively. The emission intensity ratio ($(I_o - I)/I_o$) is linearly proportional to the concentration of ATP within the range from 0 to 2.5 μM (R^2 = 0.996) (Figure 2b), and the detection limit for ATP is 27 nM (3σ/slope). Moreover, we also examined the effect of different pH values on the fluorescent responses of PMTPP to ATP. As shown in Figure S2, upon addition of 5 μM ATP, the fluorescence intensity decreased 2.8-fold, 3.3-fold, 4.0-fold, 2.7-fold, and 3.6-fold in solutions of pH 5.0, 6.0, 7.4, 8.0, and 9.0, respectively, indicating that PMTPP possesses a good response capability to ATP at a wide range of pH values.

Sensing Mechanism for ATP. Water-soluble polythiophene derivatives are fluorescent with random-coil conformation in aqueous solution, and the polymer aggregation induced by analytes through electrostatic and hydrophobic cooperative interactions results in fluorescence quenching because of $\pi-\pi$ stacking of the polythiophene backbone.[68,69] Therefore, the conformation of PMTPP was investigated with transmission electron microscopy. As shown in Figure 3a, PMTPP exhibits random-coil conformation in aqueous solution. It can aggregate upon interacting with ATP (Figure 3b). These results indicate that ATP can induce the aggregation of PMTPP through electrostatic interaction and hydrophobic cooperative interaction. At the same time, the fluorescence of the probe is quenched due to the polymer conformation changing from random-coil to aggregates.

DOI: 10.1021/acs.analchem.7b01212
Anal. Chem. 2017, 89, 8816−8821

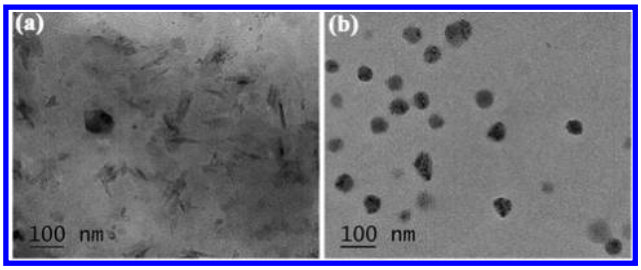

Figure 3. TEM images of PMTPP (a) and PMTPP/ATP complex (b). [PMTPP] = 100 μM, [ATP] = 10 μM.

Cytotoxicity of PMTPP. In order to assess the biocompatibility of the polymer, the toxicity of PMTPP was assayed using a MTT method. As shown in Figure 4, PMTPP does not display obvious toxicity on living cells, which indicates that PMTPP has low cytotoxicity and is favorable for biological imaging.

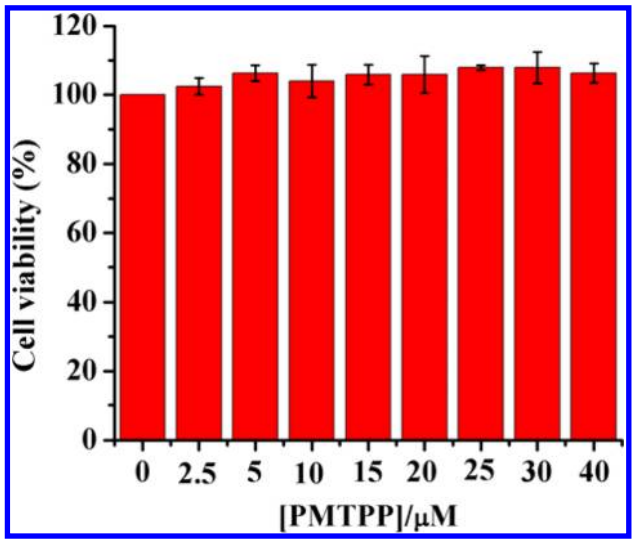

Figure 4. Cytotoxicity of PMTPP on HepG2 cells determined by MTT assays.

Membrane-Targeting Ability and Photostability of PMTPP. Colocalization experiments involving PMTPP were carried out to assess the membrane-targeting specificity of the polmer by using a confocal laser scanning microscope (CLSM). HepG2 cells and HeLa cells were costained with PMTPP and DiI (a commercially available red membrane dye). As shown in Figures 5a and S3, the green emission from PMTPP merges well with the red emission from DiI (overlap coefficient: 0.72), suggesting that PMTPP was mostly accumulated in the cell membrane. To further investigate the membrane targeting ability of PMTPP, flow cytometry experiments were employed. As shown in Figure 5b, there was a remarkable fluorescence intensity enhancement in living cells stained with PMTPP compared to the cells that were not stained with PMTPP. These results provide strong evidence that PMTPP was located on the cell membrane. Except for cancer cells, normal HL 7702 cells were stained with PMTPP. Confocal microscopy analysis showed that PMTPP was also located on the cell membrane (Figure S4). In addition, the fluorescence of PMTPP is stable in cell membranes, and the fluorescence loss of the polymer is less than 16% after 16 scans with a total irradiation time of 30 min (Figure S5). Hence, PMTPP can be used as a specific

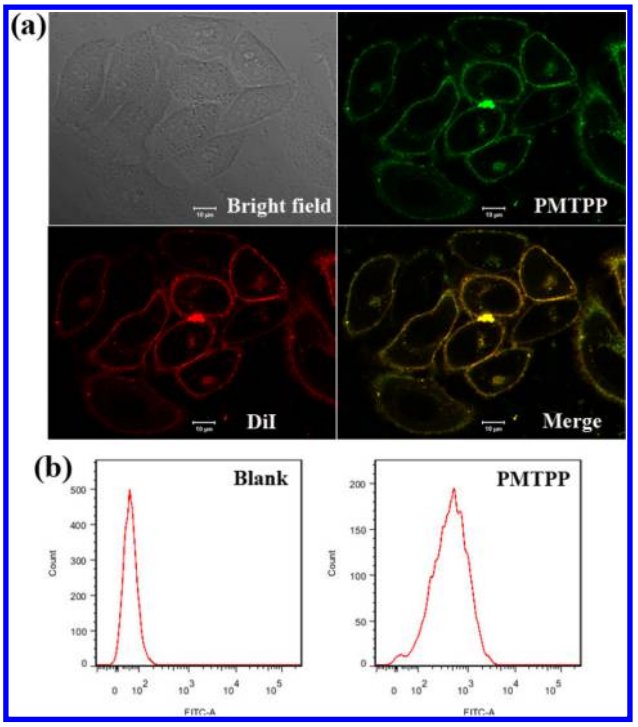

Figure 5. (a) Colocalization of HepG2 cells stained with PMTPP (15 μM) (λ_{ex} = 488 nm, λ_{em} = 500−600 nm) and DiI (10 μM) (λ_{ex} = 514 nm, λ_{em} = 530−620 nm). Scale bars: 10 μm. (b) Flow cytometry analysis of living cells stained with PMTPP (15 μM).

fluorescent agent for plasma membrane imaging and is applicable for all types of cells.

Fluorescence Imaging of ATP in Cell Membranes. We examined the applicability of PMTPP to detect ATP in cell membranes. HepG2 cells stained with PMTPP were treated with 500 μM ATP. After 22 min, the fluorescence within the cell membrane was obviously quenched (Figure S6), suggesting that PMTPP can sense ATP in the plasma membrane.

To demonstrate the capability of PMTPP to monitor changes in ATP levels in cell membranes, cisplatin was utilized to induce apoptosis. HepG2 cells stained with PMTPP were incubated with cisplatin (20 μM). During 20 min of apoptotic stimuli, the fluorescence in cell membranes was gradually quenched (Figure 6, Video S1) and a 48% of fluorescence loss was observed (Figure S7). After 40 min, the fluorescence within the cell membrane was almost unchanged (Figure S8). This result was also confirmed by flow cytometry analysis (Figure S9). To confirm the apoptotic process, Western blot experiments were used to detect caspase-3 in HepG2 cells under the stimuli of cisplatin. Caspase-3 is believed to play the role of executioner farthest downstream in apoptotic pathways, as it is commonly activated in cells by various death stimuli.[70] As shown in Figure S10, caspase-3 was obviously expressed when HepG2 cells were treated with cisplatin for 1 h. The above results indicated that the ATP levels in the plasma membrane increased during the apoptotic cell death process.

Visualization of ATP in Vivo. We also demonstrated the capability of PMTPP to monitor ATP levels in living animals. HepG2 tumor-bearing nude mice were subcutaneously injected with PMTPP near the tumor tissue and then were given an i.p. cavity injection with cisplatin for 30 min. As shown in Figure 7a, the tumor tissue showed strong fluorescence of the probe when the mice were injected with PMTPP. After the injection

DOI: 10.1021/acs.analchem.7b01212
Anal. Chem. 2017, 89, 8816−8821

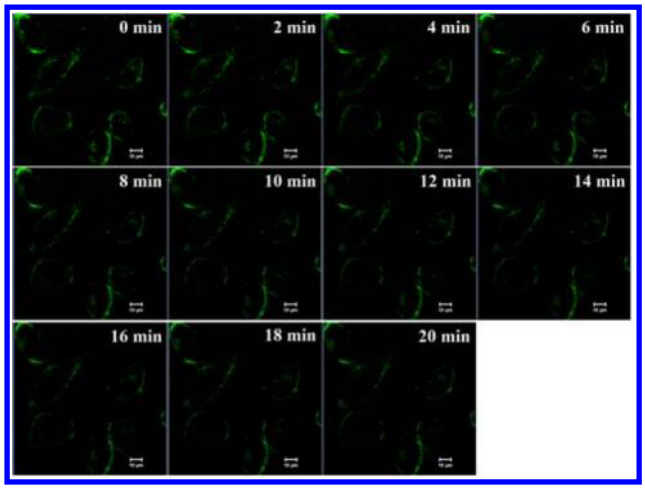

Figure 6. Time-lapse fluorescence images of HepG2 cells stained with PMTPP (15 μM) (λ_{ex} = 488 nm, λ_{em} = 500−600 nm) and then incubated with cisplatin (20 μM). Scale bars: 10 μm.

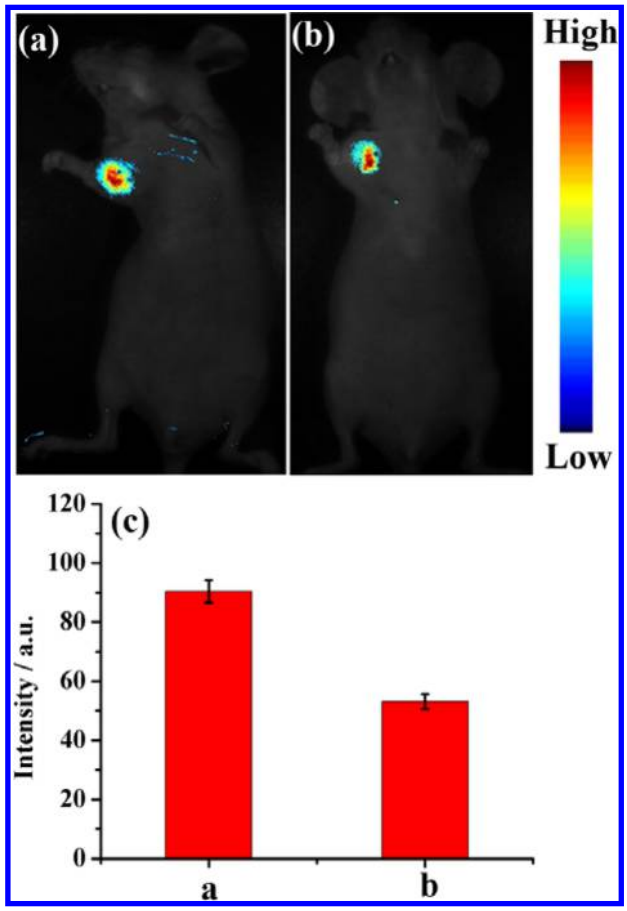

Figure 7. In vivo fluorescence images visualizing ATP levels in HepG2 tumor-bearing nude mice using PMTPP. (a) Mice were subcutaneously injected with PMTPP (250 μM, 100 μL in saline). (b) Mice were subcutaneously injected with PMTPP (250 μM, 100 μL in saline) and then were given an i.p. cavity injection with cisplatin (20 μM, 200 μL in saline) for 30 min. (c) Relative fluorescence intensity of (a) and (b).

of cisplatin for 30 min, the fluorescence within tumor tissue was obviously quenched (Figure 7b) and a 41% decrease in fluorescence intensity was observed (Figure 7c), suggesting that the ATP levels in the tumor tissue increased responding to the cisplatin stimuli. The above results confirm that PMTPP can sense ATP in mice and is favorable for imaging in vivo.

CONCLUSIONS

In summary, we synthesized a new water-soluble cell-membrane-targeting polythiophene derivative that can be utilized as a fluorescent sensor for detecting ATP in the plasma membrane. PMTPP has high sensitivity and good selectivity to ATP at physiological pH values with low detection limit. The polymer possesses low toxicity to live cells and excellent photostability in cell membranes. PMTPP has been practically applied to real-time monitoring of ATP levels in cell membranes by using fluorescence microscopy. More importantly, we found that the ATP levels in cell membranes increased during the apoptotic cell death process. In addition, the probe was also successfully utilized to image the tumor ATP levels in living mice.

ASSOCIATED CONTENT

Supporting Information

The Supporting Information is available free of charge on the ACS Publications website at DOI: 10.1021/acs.analchem.7b01212.

Synthetic route of the polymer and supplementary data, including fluorescence sensing selectivity and response, colocalization imaging of HeLa cells, fluorescence images, photostability of PMTPP, flow cytometry analysis of HepG2 cells, and Western blot analysis (PDF)

Video S1 showing the fluorescence in cell membranes being gradually quenched during 20 min of apoptotic stimuli (AVI)

AUTHOR INFORMATION

Corresponding Authors

*Fax: +86-25-89687761. E-mail: gengzr@nju.edu.cn.

*Fax: +86-25-89687761. E-mail: wangzl@nju.edu.cn.

ORCID

Zhilin Wang: 0000-0002-8123-1016

Notes

The authors declare no competing financial interest.

ACKNOWLEDGMENTS

We are thankful for support from the National Basic Research Program of China (2013CB922102) and the National Natural Science Foundation of China (21475059 and 21527809) and the Program for Outstanding PhD Candidate of Nanjing University.

REFERENCES

(1) Pérez-Ruiz, T.; Martínez-Lozano, C.; Tomás, V.; Martín, J. *Anal. Bioanal. Chem.* **2003**, *377*, 189−194.

(2) Mo, R.; Jiang, T.; DiSanto, R.; Tai, W.; Gu, Z. *Nat. Commun.* **2014**, *5*, 3364.

(3) Mo, R.; Jiang, T.; Gu, Z. *Angew. Chem., Int. Ed.* **2014**, *53*, 5815−5820.

(4) Phillips, R.; Ursell, T.; Wiggins, P.; Sens, P. *Nature* **2009**, *459*, 379−385.

(5) Hedin, L. E.; Illergård, K.; Elofsson, A. *J. Proteome Res.* **2011**, *10*, 3324−3331.

(6) Poulsen, H.; Khandelia, H.; Morth, J. P.; Bublitz, M.; Mouritsen, O. G.; Egebjerg, J.; Nissen, P. *Nature* **2010**, *467*, 99−102.

DOI: 10.1021/acs.analchem.7b01212
Anal. Chem. 2017, 89, 8816−8821

(7) Olesen, C.; Picard, M.; Winther, A. L.; Gyrup, C.; Morth, J. P.; Oxvig, C.; Møller, J. V.; Nissen, P. *Nature* **2007**, *450*, 1036−1042.
(8) Burton, B. M.; Marquis, K. A.; Sullivan, N. L.; Rapoport, T. A.; Rudner, D. Z. *Cell* **2007**, *131*, 1301−1312.
(9) Mohan, S.; Sheena, A.; Poulose, N.; Anilkumar, G. *PLoS One* **2010**, *5*, e14217.
(10) Zamaraeva, M. V.; Sabirov, R. Z.; Maeno, E.; Ando-Akatsuka, Y.; Bessonova, S. V.; Okada, Y. *Cell Death Differ.* **2005**, *12*, 1390−1397.
(11) Wang, L.; Yuan, L.; Zeng, X.; Peng, J.; Ni, Y.; Er, J. C.; Xu, W.; Agrawalla, B. K.; Su, D.; Kim, B.; Chang, Y. *Angew. Chem., Int. Ed.* **2016**, *55*, 1773−1776.
(12) Schneider, S. E.; O'Neil, S. N.; Anslyn, E. V. *J. Am. Chem. Soc.* **2000**, *122*, 542−543.
(13) McCleskey, S. C.; Griffin, M. J.; Schneider, S. E.; McDevitt, J. T.; Anslyn, E. V. *J. Am. Chem. Soc.* **2003**, *125*, 1114−1115.
(14) Butterfield, S. M.; Waters, M. L. *J. Am. Chem. Soc.* **2003**, *125*, 9580−9581.
(15) Sazani, P. L.; Larralde, R.; Szostak, J. W. *J. Am. Chem. Soc.* **2004**, *126*, 8370−8371.
(16) Cho, E. J.; Yang, L. T.; Levy, M.; Ellington, A. D. *J. Am. Chem. Soc.* **2005**, *127*, 2022−2023.
(17) Wang, J.; Jiang, Y. X.; Zhou, C. S.; Fang, X. H. *Anal. Chem.* **2005**, *77*, 3542−3546.
(18) Das, B. K.; Tlili, C.; Badhulika, S.; Cella, L. N.; Chen, W.; Mulchandani, A. *Chem. Commun.* **2011**, *47*, 3793−3795.
(19) Zhao, M.; Liao, L.; Wu, M.; Lin, Y.; Xiao, X.; Nie, C. *Biosens. Bioelectron.* **2012**, *34*, 106−111.
(20) Liu, S.; Wang, Y.; Zhang, C.; Lin, Y.; Li, F. *Chem. Commun.* **2013**, *49*, 2335−2337.
(21) Kong, L.; Xu, J.; Xu, Y.; Xiang, Y.; Yuan, R.; Chai, Y. *Biosens. Bioelectron.* **2013**, *42*, 193−197.
(22) Liu, Z.; Chen, S.; Liu, B.; Wu, J.; Zhou, Y.; He, L.; Ding, J.; Liu, J. *Anal. Chem.* **2014**, *86*, 12229−12235.
(23) Song, Y.; Yang, X.; Li, Z.; Zhao, Y.; Fan, A. *Biosens. Bioelectron.* **2014**, *51*, 232−237.
(24) Xu, Y.; Xu, J.; Xiang, Y.; Yuan, R.; Chai, Y. *Biosens. Bioelectron.* **2014**, *51*, 293−296.
(25) Wang, K.; Liao, J.; Yang, X.; Zhao, M.; Chen, M.; Yao, W.; Tan, W.; Lan, X. *Biosens. Bioelectron.* **2015**, *63*, 172−177.
(26) Wei, Y.; Chen, Y.; Li, H.; Shuang, S.; Dong, C.; Wang, G. *Biosens. Bioelectron.* **2015**, *63*, 311−316.
(27) Huo, Y.; Qi, L.; Lv, X.; Lai, T.; Zhang, J.; Zhang, Z. *Biosens. Bioelectron.* **2016**, *78*, 315−320.
(28) Zhu, Y.; Hu, X.; Shi, S.; Gao, R.; Huang, H.; Zhu, Y.; Lv, X.; Yao, T. *Biosens. Bioelectron.* **2016**, *79*, 205−212.
(29) Ma, C.; Yang, X.; Wang, K.; Tang, Z.; Li, W.; Tan, W.; Lv, X. *Anal. Biochem.* **2008**, *372*, 131−133.
(30) Lu, C.; Zhang, X.; Kong, R.; Yang, B.; Tan, W. *J. Am. Chem. Soc.* **2011**, *133*, 11686−11691.
(31) Ma, C.; Tang, Z.; Wang, K.; Yang, X.; Tan, W. *Analyst* **2013**, *138*, 3013−3017.
(32) Lin, C.; Cai, Z.; Wang, Y.; Zhu, Z.; Yang, C.; Chen, X. *Anal. Chem.* **2014**, *86*, 6758−6762.
(33) Lin, C.; Chen, Y.; Cai, Z.; Zhu, Z.; Jiang, Y.; Yang, C. J.; Chen, X. *Biosens. Bioelectron.* **2015**, *63*, 562−565.
(34) He, H.; Ma, V. P.; Leung, K.; Chan, D. S.; Yang, H.; Cheng, Z.; Leung, C.; Ma, D. *Analyst* **2012**, *137*, 1538−1540.
(35) Leung, K.; Lu, L.; Wang, M.; Mak, T.; Chan, D. S.; Tang, F.; Leung, C.; Kwan, H.; Yu, Z.; Ma, D. *PLoS One* **2013**, *8*, e77021.
(36) Quang, D.; Kim, J. S. *Chem. Rev.* **2010**, *110*, 6280−6301.
(37) Zhou, Y.; Xu, Z.; Yoon, J. *Chem. Soc. Rev.* **2011**, *40*, 2222−2235.
(38) Yuan, L.; Lin, W.; Zheng, K.; He, L.; Huang, W. *Chem. Soc. Rev.* **2013**, *42*, 622−661.
(39) Liu, Z.; He, W.; Guo, Z. *Chem. Soc. Rev.* **2013**, *42*, 1568−1600.
(40) Li, X.; Gao, X.; Shi, W.; Ma, H. *Chem. Rev.* **2014**, *114*, 590−659.
(41) Zhang, X.; Yin, J.; Yoon, J. *Chem. Rev.* **2014**, *114*, 4918−4959.
(42) Kurishita, Y.; Kohira, T.; Ojida, A.; Hamachi, I. *J. Am. Chem. Soc.* **2012**, *134*, 18779−18789.
(43) Srivastava, P.; Razi, S. S.; Ali, R.; Srivastav, S.; Patnaik, S.; Srikrishna, S.; Misra, A. *Biosens. Bioelectron.* **2015**, *69*, 179−185.
(44) Tan, K.; Li, C.; Li, Y.; Fei, J.; Yang, B.; Fu, Y.; Li, F. *Anal. Chem.* **2017**, *89*, 1749−1756.
(45) Huang, B.; Geng, Z.; Ma, X.; Zhang, C.; Zhang, Z.; Wang, Z. *Biosens. Bioelectron.* **2016**, *83*, 213−220.
(46) Ho, H. A.; Boissinot, M.; Bergeron, M. G.; Corbeil, G.; Doré, K.; Boudreau, D.; Leclerc, M. *Angew. Chem., Int. Ed.* **2002**, *41*, 1548−1551.
(47) Nilsson, K. P. R.; Inganäs, O. *Nat. Mater.* **2003**, *2*, 419−424.
(48) Doré, K.; Dubus, S.; Ho, H. A.; Lévesque, I.; Brunette, M.; Corbeil, G.; Boissinot, M.; Boivin, G.; Bergeron, M. G.; Boudreau, D.; Leclerc, M. *J. Am. Chem. Soc.* **2004**, *126*, 4240−4244.
(49) Ho, H. A.; Doré, K.; Boissinot, M.; Bergeron, M. G.; Tanguay, R. M.; Boudreau, D.; Leclerc, M. J. *J. Am. Chem. Soc.* **2005**, *127*, 12673−12676.
(50) Najari, A.; Ho, H. A.; Gravel, J. F.; Nobert, P.; Boudreau, D.; Leclerc, M. *Anal. Chem.* **2006**, *78*, 7896−7899.
(51) Ho, H. A.; Leclerc, M. *J. Am. Chem. Soc.* **2004**, *126*, 1384−1387.
(52) Béra Abérem, M.; Najari, A.; Ho, H. A.; Gravel, J. F.; Nobert, P.; Boudreau, D.; Leclerc, M. *Adv. Mater.* **2006**, *18*, 2703−2707.
(53) Yao, Z. Y.; Ma, W. J.; Yang, Y.; Chen, X. L.; Zhang, L.; Lin, C.; Wu, H. C. *Org. Biomol. Chem.* **2013**, *11*, 6466−6469.
(54) Ho, H. A.; Leclerc, M. *J. Am. Chem. Soc.* **2003**, *125*, 4412−4413.
(55) Li, C.; Numata, M.; Takeuchi, M.; Shinkai, S. *Angew. Chem., Int. Ed.* **2005**, *44*, 6371−6374.
(56) Yao, Z.; Li, C.; Shi, G. *Langmuir* **2008**, *24*, 12829−12835.
(57) Yao, Z. Y.; Feng, X. L.; Li, C.; Shi, G. Q. *Chem. Commun.* **2009**, 5886−5888.
(58) Yao, Z. Y.; Bai, H.; Li, C.; Shi, G. Q. *Chem. Commun.* **2011**, *47*, 7431−7433.
(59) Wang, X.; Feng, Q.; Wang, L.; Pei, M.; Zhao, J.; Zhang, G. *Des. Monomers Polym.* **2014**, *17*, 26−32.
(60) Cheng, D.; Li, Y.; Wang, J.; Sun, Y.; Jin, L.; Li, C.; Lu, Y. *Chem. Commun.* **2015**, *51*, 8544−8546.
(61) Chen, Z.; Wu, P.; Cong, R.; Xu, N.; Tan, Y.; Tan, C.; Jiang, Y. *ACS Appl. Mater. Interfaces* **2016**, *8*, 3567−3574.
(62) Wang, B.; Zhu, C.; Liu, L.; Lv, F.; Yang, Q.; Wang, S. *Polym. Chem.* **2013**, *4*, 5212−5215.
(63) Tang, H.; Xing, C.; Liu, L.; Yang, Q.; Wang, S. *Small* **2011**, *7*, 1464−1470.
(64) Xing, C.; Liu, L.; Tang, H.; Feng, X.; Yang, Q.; Wang, S.; Bazan, G. C. *Adv. Funct. Mater.* **2011**, *21*, 4058−4067.
(65) Wang, F.; Li, M.; Wang, B.; Zhang, J.; Cheng, Y.; Liu, L.; Lv, F.; Wang, S. *Sci. Rep.* **2015**, *5*, 7617−7621.
(66) Qian, C.; Yu, J.; Chen, Y.; Hu, Q.; Xiao, X.; Sun, W.; Wang, C.; Feng, P.; Shen, Q.; Gu, Z. *Adv. Mater.* **2016**, *28*, 3313−3320.
(67) Zhu, H.; Fan, J.; Du, J.; Peng, X. *Acc. Chem. Res.* **2016**, *49*, 2115−2126.
(68) Feng, X.; Liu, L.; Wang, S.; Zhu, D. *Chem. Soc. Rev.* **2010**, *39*, 2411−2419.
(69) Zhu, C.; Liu, L.; Yang, Q.; Lv, F.; Wang, S. *Chem. Rev.* **2012**, *112*, 4687−4735.
(70) Jänicke, R. U.; Ng, P.; Sprengart, M. L.; Porter, A. G. *J. Biol. Chem.* **1998**, *273*, 15540−15545.

DOI: 10.1021/acs.analchem.7b01212
Anal. Chem. 2017, 89, 8816−8821